



# A prediction of axial capacity of rectangular concrete filled steel tube columns using neural network

Ali Abdullah Hassooni<sup>a</sup> and Hussein Yousif Aziz<sup>a</sup>

<sup>a</sup>Department of Civil Engineering, College of Engineering, Al-Muthanna University, Samawah, Iraq

\*Corresponding author E-mail: [ali.abdullah1230@gmail.com](mailto:ali.abdullah1230@gmail.com)

DOI:10.52113/3/eng/mjet/2023-11-02/09-29

## Abstract

In recent decades, Concrete filled steel tube (CFST) columns have been widely utilized in construction due to their high strength, ductility, energy absorption, fire resistance, and cost reduction due to the absence of formwork. Estimating the Axial compressive capacity (ACC) of short rectangular CFST columns has been the subject of numerous experiments. In this study, artificial neural network was used to make predictions regarding the ACC of CFST columns. Multi fed forward back propagation and Adaptive neuro fuzzy inference system were used. 512 experimental tests were collected from the literature. One thousand models for multi fed forward back propagation and one hundred for adaptive neuro fuzzy inference system were trained and tested. artificial neural network models are evaluated by using statistical analysis to validate and test the prediction models. The best models were selected by using the Root mean square error (RMSE) and Coefficient of determination ( $R^2$ ). Using the RMSE,  $R^2$ , and Mean absolute percentage error (MAPE), the best models were compared to design code formulas. As a result, the best model performed much better in every performance measure. The best model for multi fed forward back propagation has better performance in comparison with the best model for adaptive neuro fuzzy inference system. For interested users and researchers, a graphical user interface was created using the best model for multi fed forward back.

**Keywords:** Artificial neural network, Multi fed forward back propagation, Adaptive neuro fuzzy inference system, Concrete filled steel tube columns, Axial compressive capacity.

## 1. Introduction

Steel-concrete composite columns come in two varieties that are commonly utilized in structures. Those with concrete-filled steel sections and those with concrete-encased steel sections, as indicated in Figure 1 [1, 2]. Amazing characteristics of the Concrete filled steel tube (CFST) Structural System include its high strength, high ductility, high lateral stiffness, energy absorption, damping against vibration, fire resistance, and significant time savings during construction because formwork is not required. A CFST member is made up of two materials that have different stress-strain curves and behave differently. Because of the interactions between the two materials, determining combined properties such as second moment and elastic modulus is difficult. The failure mode is heavily influenced by the cross-section area, steel percentage, and concrete and steel strength. Contact between steel and concrete, concrete confinement, residual stresses, creep, shrinkage, and loading type all have an impact on the behavior of CFST columns. Despite its many advantages, the adoption of CFST in building construction has been hampered by a lack of knowledge regarding construction and the difficulty of connection detailing. More analysis and research are required to ensure that this technology can be used in construction without causing difficulties [1, 2]. High-rise buildings, bridge piers with high traffic strain rates, and railway decks use CFST columns for earthquake resistance. Furthermore, as compared to concrete encased steel composite sections, CFST columns exhibit strong compressive and torsional resistance along all axes [2, 3]. The load was divided into concrete and steel at the beginning of the loading process. The confinement effect begins to occur during the following phase of loading. The concrete becomes subject to triaxial stresses, whereas steel is subject to biaxial stresses. Some researchers, such as Knowles and Park, reported that concrete confinement abruptly occurs around  $0.95 f_c$  (strain of 0.002), when the concrete begins to expand [4]. Tsuji et al. and Zhang et al. recommended a steady rise in concrete confinement

starting with microcracking in the concrete (strain of 0.001) and progressing to 100% confinement is achieved at a strain of around 0.002 [5, 6]. Failure modes of the CFST can vary widely based on the material characteristics and geometric configuration of the component parts. Most steel tubes fail due to local buckling. In comparison to an empty steel tube, the existence of concrete infill delays local buckling in the CFST column. The concrete prevents the steel tube from bending inward, as shown in Figure 2. Instead, the concrete makes it buckle outward [7]. The shape of the CFST columns is determined by the geometry of the steel tube it is contained in, therefore it might be round, square, rectangular, L-shaped, elliptical, etc. In the construction field, square and circular CFST sections are utilized the most frequently. The load carrying capability of a CFST column is greatly influenced by its cross-section shape, as well as the steel tube's length-to-thickness ratios [1, 8, 9].

In 1901, Sewell did the first research study on CFST columns, and in 1957, Kloppel and Goder did the first thorough test on CFST columns [10, 11]. In Sewell's investigation, the reason the hollow tube inside the tube column was filled with concrete was to keep it from rusting. After some of the columns were accidentally overloaded, the stiffness of the structure improved noticeably. Kloppel and Goder tested the first column in the late 1970s; since then, research into the Axial compressive capacity (ACC) of CFST columns has advanced dramatically [10].

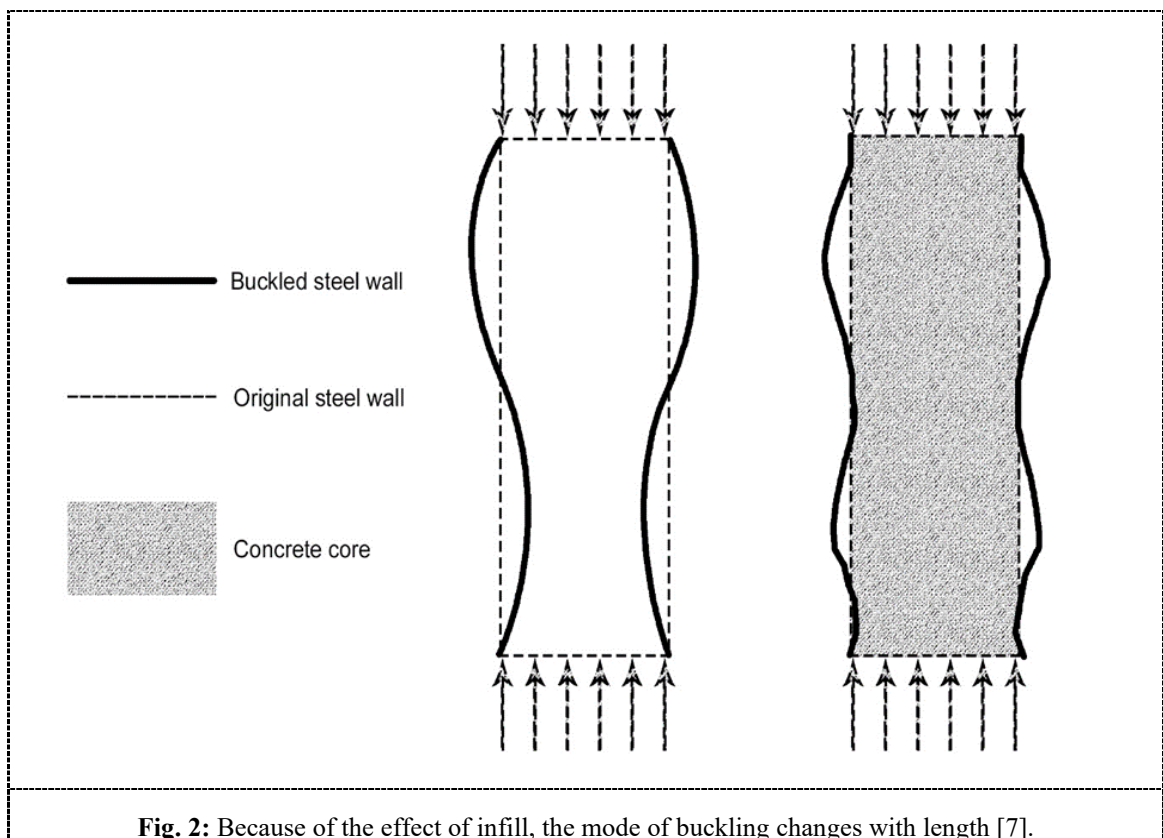
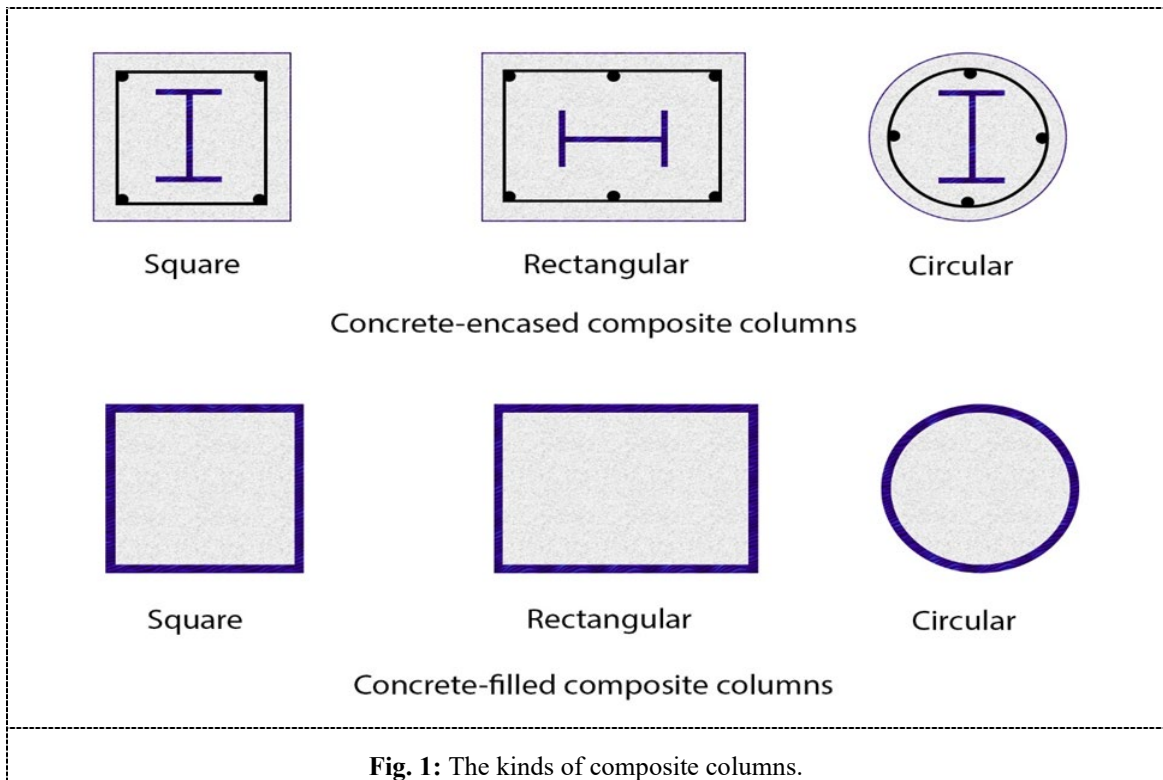
Artificial neural networks were initially conceived of being straightforward representations of how brains work. There are billions of neurons in the human brain, all of which are interconnected. These are cells that contain particular members that make it possible for single to be communicated to the neurons that are located nearby [12].

Observations of the application of prediction networks in civil engineering may be found in the works of French et al. [13], Kasperkiewicz et al. [14], Grubert [15], Aziz [16], Thirumalaiah and Deo [17], Deo and Kumar [18], Jiang et al. [19], Jakubek and Strasser [20] and Zhao [21], amongst others. Over the past few years, a number of computational research that make use of artificial intelligence and machine learning methodologies have seen widespread application. Several studies have used methods like artificial neural network, gene-expression programming, particle swarm optimization, and the imperial competitive algorithm for civil engineering. Some of these sources include Armaghani et al. [22], Chen et al. [23], Parsajoo et al. [24], Du et al. [25], Kovačević et al. [26], Li et al. [27], Asteris et al. [28], Nguyen et al. [29], Armaghani et al. [30], Asteris et al. [31], Asteris et al. [32] and Khajehzadeh et al. [33].

The ACC of CFST columns was predicted using artificial neural network by Moon et al. [34], Ahmadi et al. [35], Ahmadi et al. [36], Du et al. [37], Jayalekshmi et al. [38], Tran et al. [39], Tran et al. [40], Zarringol et al. [41], Asteris et al. [42], Sarir et al. [43], Le et al. [44], Luat et al. [45], Mai et al. [46], Avci-Karatas [47], Wang and Chan [48], Duong et al. [49] and Zhou et al. [50]. It should be noted that the majority of studies only attempted to estimate the ACC of CFST columns under axial force. In addition, the networks were trained with insufficient data, which limits artificial neural networks' ability to learn input-output correlations over many ranges and hence reduces prediction accuracy. All of the previous studies used one or two hidden layers and not more than 25 neurons in each hidden layer. In addition, three activation functions were used: Hyperbolic tangent sigmoid, Log-sigmoid, and Linear transfer function. On the other hand, most of studies focused just on developing artificial neural networks without producing any graphical user interface or empirical equation from the trained networks.

In construction, CFST columns have been used a lot in the last few decades. Despite the fact that CFST columns are structurally vulnerable to bending, shear, and torsion, their ACC remains a significant aspect of their design. The design codes and mathematical model that were proposed by the authors for predicting the ACC of CFST columns are unable to accurately estimate the ACC of CFST columns, as will be mentioned later. As well as limitations for application, it is concerned with the use of strong strength materials steel and concrete.

In the current investigation, an artificial neural network was utilized to make predictions regarding the ACC of short rectangular CFST columns. For the purpose of generalizing the link between inputs and outputs, experimental tests were taken from the published research and used to train the artificial neural network. In this study, the artificial neural network models were made with more than hidden layers, neurons, and another activation function. Using an adaptive neuro fuzzy inference system model, the ACC of CFST columns was predicted. The model that makes the best predictions was chosen. In the end, a graphical user interface was designed by making use of the most effective model.



### 1.1. Design codes

The ACC estimation of CFST columns is supported by a number of design standards for steel and composite members. These include Eurocode4[51], AISC360[7], ACI318[52], AIJ (2001) [53], DBJ (2010) [54], AS5100 [55]. As well, almost all design codes have limits on how they can be used, such as limiting the range of strengths that can be used for steel and concrete. In addition, several codes include limitations on the amount of steel that can be contained within the composite section. Table 1 shows the deferent limitations for design codes.

**Table 1:** Limitation of design codes

Design codes	Material properties		Geometric properties	Other limitation
	$f_y$ (MPa)	$f_c$ (MPa)	Rectangular section	
Eurocode 4	$235 \leq f_y \leq 460$	$20 \leq f_c \leq 50$	$\frac{b}{t} \leq 52 \sqrt{\frac{235}{f_y}}$	$0.2 \leq \frac{A_s f_y}{N_{pl}} \leq 0.6$
AISC 360 - 16	$f_y \leq 525$	$21 \leq f_c \leq 69$	$\frac{b}{t} \leq 5 \sqrt{\frac{E_s}{f_y}}$	$\frac{A_s}{A_g} \leq 0.01$
AS 5100	$f_y \leq 350$	$25 \leq f_c \leq 65$	$\frac{b}{t} \left( \sqrt{\frac{f_y}{235}} \right) \leq 45$	
Japanese code AIJ 2001	$235 \leq f_y \leq 355$	$18 \leq f_c \leq 60$	$\frac{b}{t} \leq 1.5 \frac{735}{\sqrt{f_y}}$	
Chinese code- 2010	$235 \leq f_y \leq 420$	$24 \leq f_c \leq 70$	$\frac{L}{b} \leq 50$	
ACI318 - 2014	$f_y \leq 345$	$f_c \geq 17.2$	$\frac{H}{t} \leq 60 \left( \sqrt{\frac{235}{f_y}} \right)$	
			$\frac{H}{t} \leq \left( \sqrt{\frac{3 E_s}{f_y}} \right)$	

### 1.1.1. Eurocode 4 (2004)

The ACC of CFST columns could be estimated by employing the formula that is described in EC4 as follows:

$$N_{p1} = A_s f_y + A_c f_c \quad (1)$$

$$\text{The axial load capacity} = N_{p1} X \quad (2)$$

Where  $X$  reduction factor [51].

### 1.1.2. Figure captions

Only within certain characteristics and restrictions, the AISC-360-16 standard provides a formula that can forecast the ACC of CFST columns [7]. As the following equation demonstrates, the compressive strength of a CFST section is identical to the section's plastic strength in the event that the section is compact:

If  $\lambda \leq \lambda_p$  then  $P_{no} = P_{no1}$  compact section

If  $\lambda_p < \lambda \leq \lambda_r$  then  $P_{no} = P_{no2}$  non-compact section

If  $\lambda > \lambda_r$  then  $P_{no} = P_{no3}$  slender section

where  $P_{no1}$  is compact section's compressive strength,  $P_{no2}$  is non-compact section's compressive strength,  $P_{no3}$  is the slender section's compressive strength,  $\lambda_r = 3 \sqrt{\frac{E_s}{f_y}}$ ,  $\lambda_p = 2.26 \sqrt{\frac{E_s}{f_y}}$ ,  $\lambda = \frac{\text{Width}}{\text{Tube thickness}}$ .

The nominal compressive strength is calculated depending on the column slenderness as follows:

$$\text{When } \frac{P_{no}}{P_e} \leq 2.25$$

where  $P_e$  is the Euler critical buckling load.

$$\text{The compressive strength} = P_{no} (0.658)^{\left(\frac{P_{no}}{P_e}\right)} \quad (3)$$

When  $\frac{P_{no}}{P_e} > 2.25$

$$\text{The compressive strength} = 0.877 P_e \quad (4)$$

### 1.1.3. ACI 316 (2014)

The ACI [52] states that, The CFST column's ACC is given by

$$P_{ACI} = A_s f_y + 0.85 A_c f_c' \quad (5)$$

Where  $A_s$  and  $A_c$  are the cross-section areas for steel and concrete, respectively,  $f_y$  represented steel's yield strength and  $f_c'$  represented concrete's compressive strength.

### 1.1.4 AS 5100 (2004)

The ACC for CFST columns is being estimated using AS 5100 [55] by combining the tube's and concrete's axial load capacities. This leads to

$$N_{pl} = \phi A_s f_y + \phi_c A_c f_c' \quad (6)$$

where  $A_s$  and  $A_c$  are the cross-section areas for steel and concrete, respectively,  $\phi$  and  $\phi_c$  are the capacity factors for steel and concrete, respectively, with values of 0.90 and 0.60 respectively.

The influence of the column's slenderness is then taken into consideration with the help of a reduction factor that is denoted by  $\alpha_c$ . As a result of this, the ACC of the column could be determined as follows:

$$N_{AS} = \alpha_c N_{pl} \quad (7)$$

Where  $\alpha_c$  the slenderness reduction factor.

### 1.1.5 Japanese codes (AIJ-2001)

According to Japanese code [53]. Use the following formula to determine ACC of CFST columns:

If  $\frac{KL}{h} \leq 4$  then the ACC is

$$N_{u1} = 0.85 f_c' A_c + (1 + \eta) f_y A_s \quad (8)$$

Where  $\eta = 0$  for a rectangular CFST column

If  $4 < \frac{KL}{h} \leq 12$ , then the ACC is

$$N_{u2} = N_{u1} - 0.125 (N_{u1} - N_{u3}) \left( \frac{L}{D \text{ or } b} - 4 \right) \quad (9)$$

If  $\frac{KL}{h} > 12$ , then the ACC is

$$N_{u3} = A_c N_b^c + N_b^s \quad (10)$$

where KL is the member's effective length,  $N_b^c$  is the buckling capacities of the concrete,  $N_b^s$  is the steel tube's buckling capacity.

### 1.1.6 DBJ 13-51 (2010)

With the assistance of a combined yield stress, which is represented by the symbol  $F_{sc}$  in the Chinese code DBJ 13 [54], the compression load that is applied to the CFST columns section may be calculated. The CFST column's compressive resistance is then calculated as:

$$N_{DBJ} = F_{sc} (A_s + A_c) \quad (11)$$

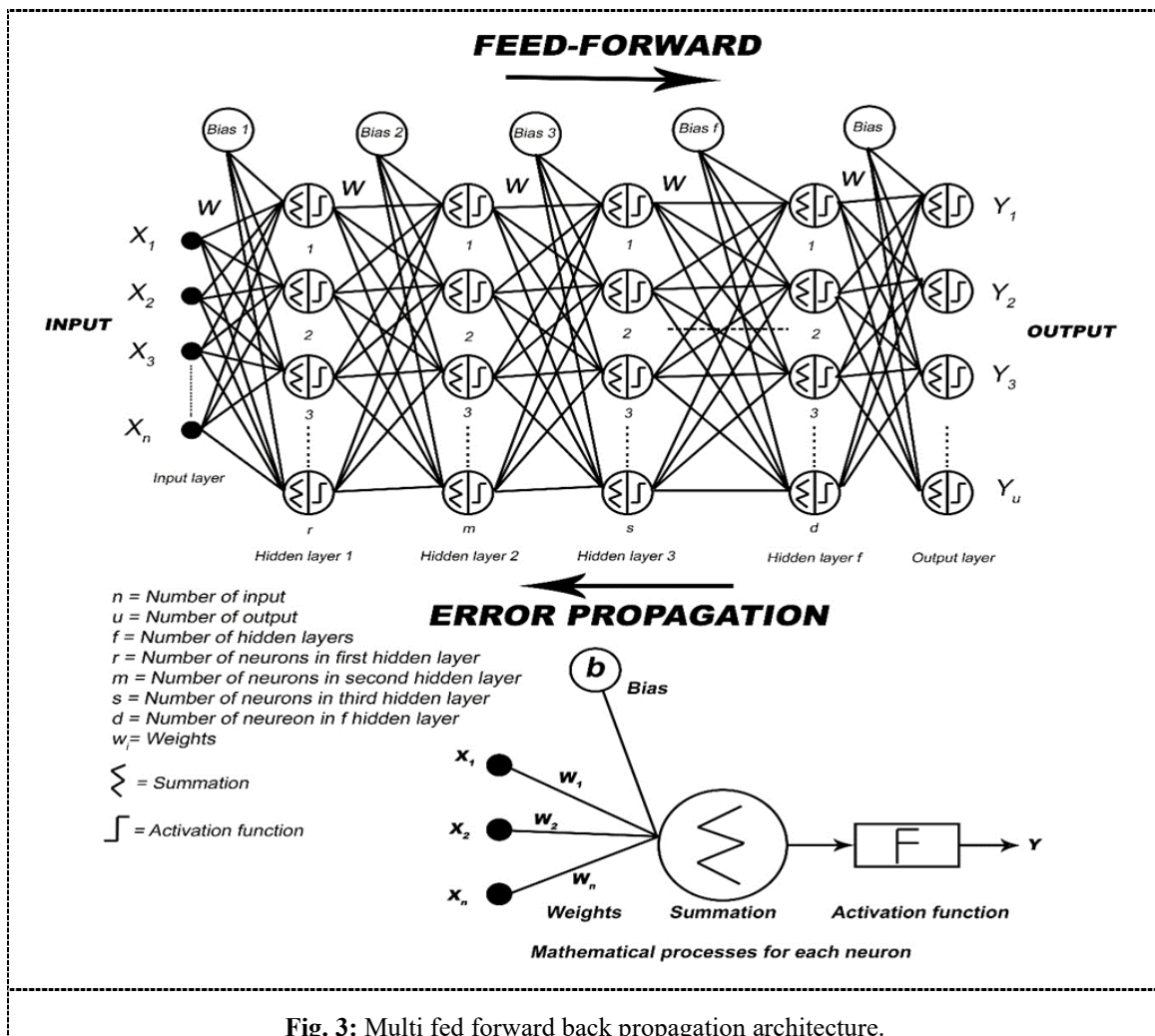
On other hand, Gourley and Hajjar [56], Zhang and Shahrooz [57] and Inai and Sakino [58] suggested a number of different methodologies for measuring the ACC of rectangular CFST columns. According to these models, confinement was assumed to increase the concrete core's ductility but not its strength. Sakino et al. provided design methods to forecast the ACC of circular or square CFST columns [59].

## 2. Neural network and neuro fuzzy modeling

### 2.1. Multi fed forward back propagation

In the early 1970s, a number of different sources introduced the feed forward, backpropagation architecture [60]. Figure 3 illustrates the back propagation architecture of a multi fed forward back propagation neural network.

The three primary elements that make up an multi fed forward back propagation neural network are the input layer, the hidden layers, and the output layer. There are a number of neurons in each layer. Neurons in the input layer are equivalent to inputs, and neurons in the output layer are equivalent to outputs. It could contain multiple layers that are hidden. Each hidden layer contains a certain number of neurons, and by applying the approach of trial and error, the ideal number of neurons can be found. Each neuron performs mathematical operations by multiplying income by weights, adding them together, and then entering the activation function to produce the neuron's output. There are several activation functions can be used. Using error back propagation, the weights were changed to make the difference between the target and predicted values small as possible. Throughout the training process, these processes keep repeating themselves. When the discrepancy between predicted and target values is reduced to the desired value, the training procedure will be complete [61, 62].



### 2.2. Adaptive neuro fuzzy inference system

The idea of fuzziness was first put forth by Zadeh (1965). He introduced fuzzy sets in order to represent complex and intricate systems using fuzzy approximation. "Generally, fuzzy logic can be considered as a logical system that provide a model for modes of human reasoning that are approximations rather than exact" [63]. The fuzzy neural network is a system that blends fuzzy logic and artificial neural networks theory [64].



Figure 4 (a) shows the membership function and (b) the architecture of the adaptive neuro fuzzy inference system. There are five main layers that make up the adaptive neuro fuzzy inference system. The first layer divided the inputs to many logics, such as long, medium, and short, by using the membership function, which is known as the fuzzification layer. There are several memberships that can be used. The generation of the rules falls under the purview of the second layer. There are two rules that can be generated: AND and OR. When the rule is AND, it means multiplying each income from the first layer together. The third layer is the ratio of rule weights to the sum weights of the rules. The fourth layer is multiplied by the normalized value and consequence parameters set for each input with the weight ratio from the previous layer. The fifth layer is a summation of the overall incomes from the fourth layer. The hybrid back propagation algorithm is used to reduce the error between the predicted values and the target values as much as possible [65].

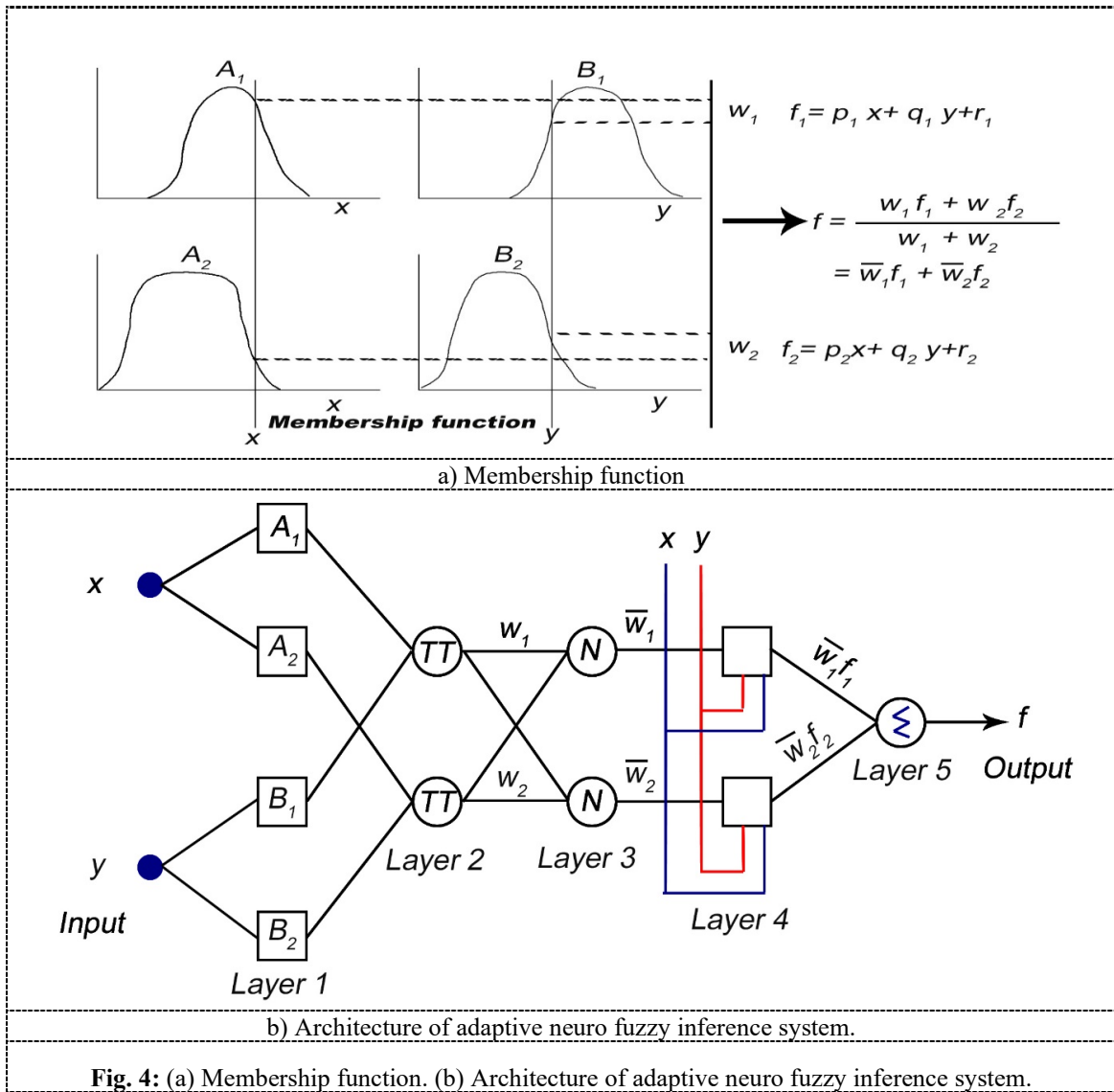
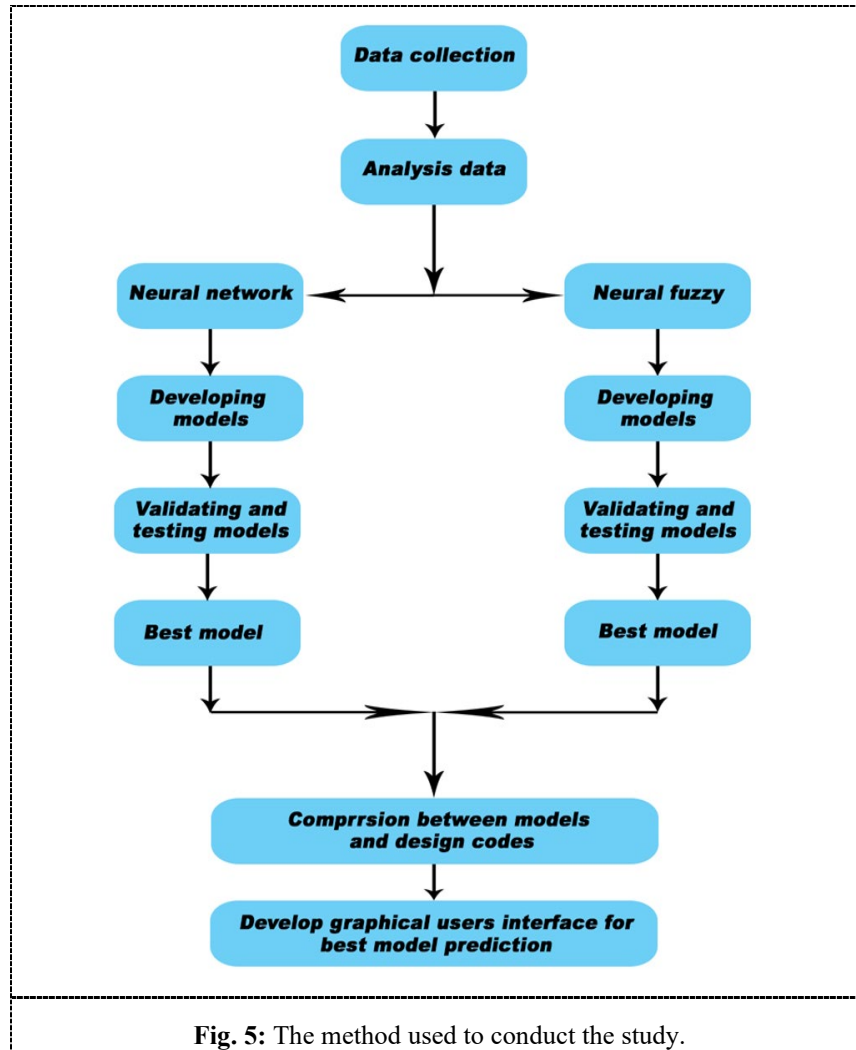


Fig. 4: (a) Membership function. (b) Architecture of adaptive neuro fuzzy inference system.

### 2.3. Methodology

The researchers describe in this part the process they used to build the artificial neural network models. Figure 5 illustrates the method used to conduct this study. To begin, experimental data was gathered from the various published sources that were available. Secondly, data analysis was performed to delete similar data. Thirdly, in order to create prediction model of the ACC of CFST columns, two different kinds of artificial neural network are utilized. Multi fed forward back propagation and adaptive neuro fuzzy inference system were used. Models were evaluated using statistical analysis to validate and test the model's prediction. The best models were selected from models that have the lowest error prediction. A comparison was made between the performance of the best models and the formulas of design codes as the fourth step in the process. Finally, it develops a graphical user interface using the best models selected for estimation of the ACC of CFST columns. The most efficient model was used to create a graphical user interface. All the work was performed by MATLAB R2020a using the live script codes.



## 2.4. Experimental datasets

On short, rectangular CFST columns, a variety of experiments were collected in order to train and build the artificial neural network models. A significant portion of the database was taken from [66] databases. The investigation entirely focused on specimens that had been subjected to a monotonic concentric load and did not contain any steel reinforcement. If a source reported the compressive cube strength of concrete ( $f_{cu}$ ), the following formula was used to convert  $f_{cu}$  to  $f'_c$  [67]:

$$f'_c = [0.76 + 0.21 \log_{10}(f_{cu}/19.6)] f_{cu} \quad (12)$$

Short CFST columns have length-to-width ratios of less than or equal to 4, whereas long CFST columns have length-to-width ratios larger than 4 [68]. Based on above expression 512 experimental tests were collected with parameters including width, height, steel tube thickness, length, steel's yield strength and concrete's compressive strength. Normal ( $f_y$  equal or less than 460 MPa and  $f'_c$  equal or less than 50 MPa) to high strengths ( $f_y$  greater than 460 MPa and  $f'_c$  greater than 50 MPa) material properties are available [51].

Table 2 presents a statistical analysis of input parameters and output, which covers the minimums and maximums as well as the mean and standard deviation. When it comes to properties of materials, it is clear that a wide variety of steel yield strength limits, including mild and high strength steels, is covered. Similarly, the database contains a wide range of concrete strengths.

Figure 6 shows the data parameters' histogram. A significant amount of research was clearly done on specimens with dimensions of 100 to 150 mm width, 80 to 220 mm height, 1.8 to 6.2 mm steel tube thickness, 200 to 700 mm length, 250 to 450 MPa steel's yield strength, 20 to 80 MPa concrete's compressive strength, 0.5 to 50 heights to tube thickness ratio, 2.8 to 3.2 length to width ratio, and 100 to 3000 kN ACC.

All parameters, input and output, are interdependent, as shown in Figure 7. Input parameters with a high coefficient imply a linear relationship between variables, reducing the database's generality. Except for the high coefficients between width and height, width and length, and height and length, the correlation coefficient for all other couples of input parameters is  $<0.6$ , indicating sufficient dispersion. The ratio of height to steel tube thickness and the ratio of length to width have the lowest correlations between input parameters and output.



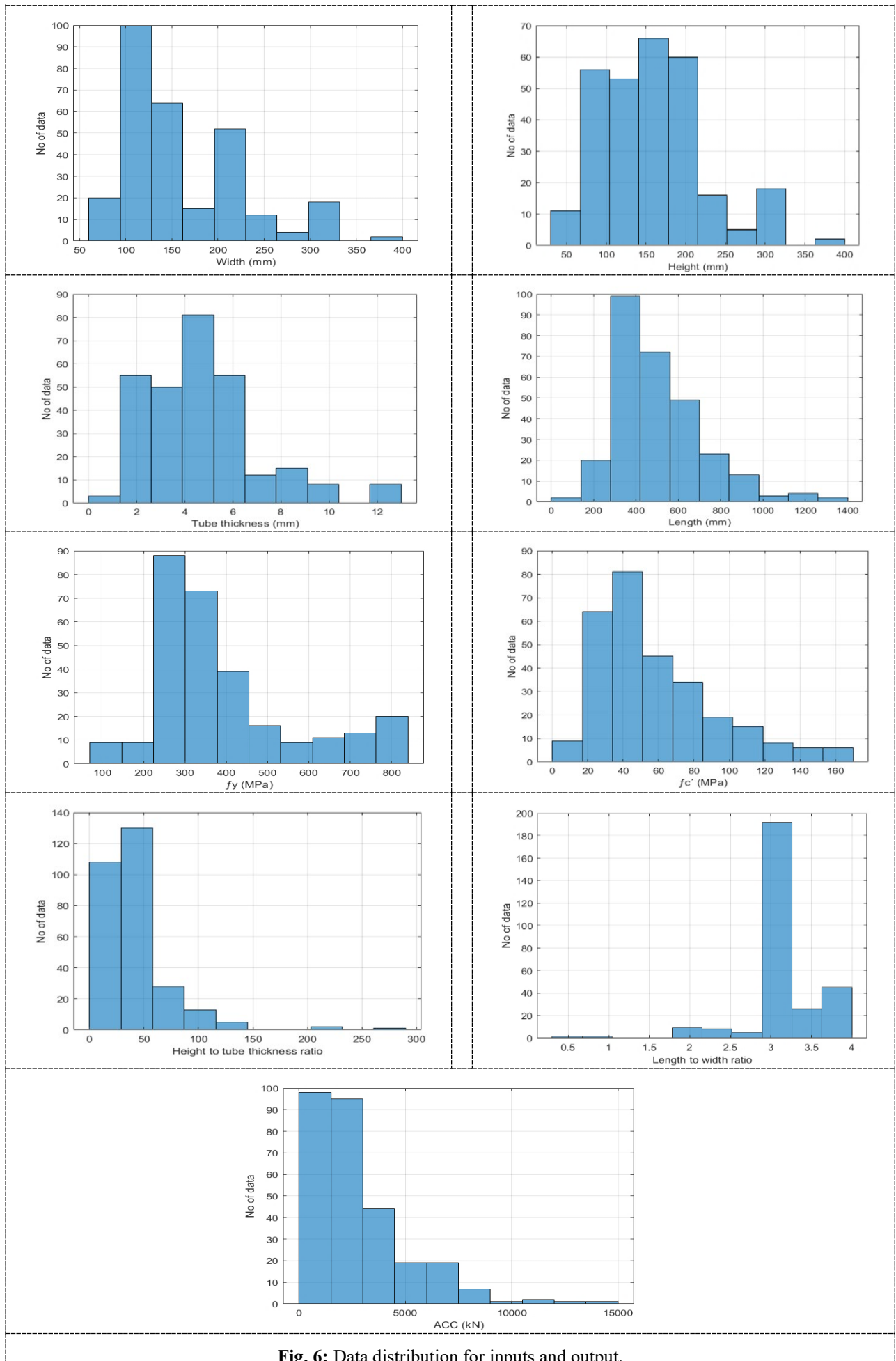
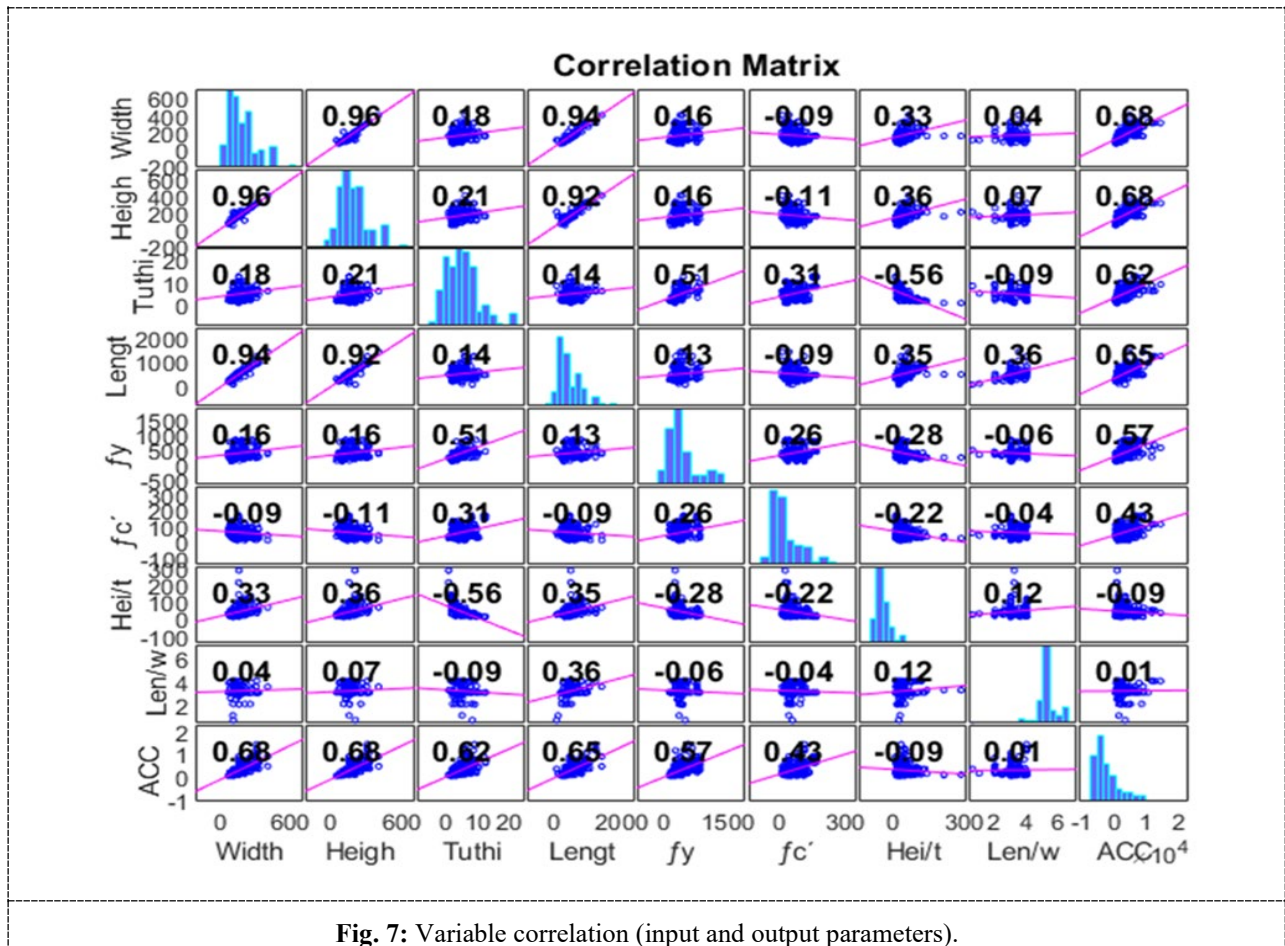


Fig. 6: Data distribution for inputs and output.



**Table 2:** Statistical analysis of data parameters.

Type of statistics function	Width (mm)	Height (mm)	Tube thickness (mm)	Length (mm)	$f_y$ (MPa)	$f_c$ (MPa)	H/t	L/b	ACC (kN)
Mean	157.96	160.56	4.77	495.41	393.28	58.51	42.42	3.13	2769.94
Min	60.00	44.00	0.70	60.00	115.00	8.52	10.49	0.59	182.00
max	400.00	400.00	12.50	1400.0	835.00	164.10	285.7	4.00	14116.00
Standard deviation	64.82	64.93	2.41	223.43	177.60	34.04	31.50	0.47	2344.61

### 3.3. Multi fed forward back propagation neural network

The parameters that were used to develop the multi fed forward back propagation are described in this section by researchers. MATLAB's artificial neural network Toolbox was used in the process of developing the networks [69]. Most of the time, multi fed forward back propagation network is the one used in engineering. As a result, this network was trained using the back-propagation approach. There are various back-propagation algorithms for training a network, including Levenberg-Marquardt and Resilient backpropagation. The algorithm chosen is influenced by a number of parameters, including the network's complexity and the number of inputs [69]. The Levenberg-Marquardt technique was used as the learning mechanism in this study. In addition, the Levenberg-Marquardt technique has the advantage of requiring a validation dataset to prevent overfitting and utilizing 70% of the data for training the neural network, 25% for validating the network, and 5% for testing the network [69]. The size of an artificial neural network is largely determined by its number of hidden layers and the number of nodes in each layer [70].

Width, height, steel tube thickness, length, steel's yield strength, and concrete's compressive strength were employed as input parameters in the development of artificial neural network models, with and without the height to tube thickness of steel ratio and the length to width ratio. The ACC of CFST columns as output of artificial neural network. Table 3 lists artificial neural network training settings. It divided the database randomly into three groups: 70% for training, 25% for validating, and 5% for testing. The input and output data are normalized between 0 and 1. Hidden layers have six different functions, and the output layer's activation function is a linear transfer function [69].

**Table 1:** Model training parameters for artificial neural networks.

Parameters	Value	MATLAB function
Training approaches	Levenberg–Marquardt function	TRAINLM
Normalize	Between (0 - 1)	MAPMINMAX
Count of layers that are hidden	(1 - 4)	
Hidden layer neurons	(5 - 10 - 15 - 20 - 25 - 30 - 35 - 40)	
Database dividing	70% for training, 25% for validating, 5% for testing	DIVIDERAND
Training goal	0	
Epochs	1000	
Cost function	Mean square error	MSE
	Hyperbolic tangent sigmoid	TANSIG
	Log-sigmoid	LOGSIG
Hidden layer's activation function	Positive linear	POSLIN
	Softmax	SOFTMAX
	Triangular basis	TRIBAS
	Radial basis	RADBAS
Output layer's transfer function	Linear	PURELIN

## 2.6. Adaptive neuro fuzzy inference system

In this section, researchers describe the parameters used to develop the adaptive neuro fuzzy inference system. The adaptive neuro fuzzy inference system model was created using the MATLAB neuro fuzzy designer toolbox. In the study, the Sugeno type of adaptive neuro fuzzy inference system, Gaussian membership function, and subtractive clustering were used to generate the rules for the adaptive neuro fuzzy inference system. Table 4 shows the parameters for training and making rules for the adaptive neuro fuzzy inference system [71]. It divided the database randomly into three groups: 70% for training, 25% for validating, and 5% for testing [71]. The parameters used to create the multi fed forward back propagation neural network are the same as those used to create it.

**Table 2:** The settings that determine how the adaptive neuro fuzzy inference system learns and creates its rules.

Parameters	Value	MATLAB function
Training algorithm	Hybrid algorithm	
Error tolerance	0	
Database dividing	70% for training, 25% for validating, 5% for testing	DIVIDERAND
Epochs	20	
Cluster influence range	(0.5 - 0.55 - 0.6 - 0.65 - 0.7)	
Squash factor	(0.2 - 0.25 - 0.3 - 0.35 - 0.4)	
Accept ratio	(0.2 - 0.3 - 0.4 - 0.5 - 0.6)	
Reject ratio	(0.15 - 0.25 - 0.35 - 0.45 - 0.55)	

## 2.7. Performance models

Three typically employed indicators, including Root mean square error (RMSE), Coefficient of determination ( $R^2$ ) and mean absolute percentage error (MAPE), are utilized in the process of performance and effectiveness evaluation. The following is the computation for these indicators:

$$RMSE = \sqrt{\frac{1}{m} \sum_{i=1}^m (p_i - y_i)^2} \quad (13)$$

$$R^2 = 1 - \frac{\sum_{i=1}^m (p_i - y_i)^2}{\sum_{i=1}^m (p_i - p_{av})^2} \quad (14)$$

$$MAPE = \frac{1}{m} \sum_{i=1}^m \left| \frac{(p_i - y_i)}{p_i} \right| \quad (15)$$

where  $p$  is the value that has been predicted,  $y$  is the value that has been targeted,  $m$  is the number of samples, and  $p_{av}$  is the average of the values that have been predicted.

The developed models' dependability and accuracy were assessed using RMSE and  $R^2$ . The RMSE is a metric that may be used to assess short-term efficiency and is a benchmark for the difference between projected values and target values. The lower RMSE, the more precise the model evaluation. The variance that the model interprets, or the variance that is reduced when employing the model, is measured by the  $R^2$ .  $R^2$  values range from (0 - 1), with the model showing good predictability when it is close to 1 and not undergoing analysis when it is close to 0. The overall prediction accuracy can be determined by these performance criteria. Regardless of whether the deviation was positive or negative, MAPE represents the average difference between the estimated and target values. The smaller MAPE, the more accurate the model evaluation.

### 2.8. Best models selection and comparison

Researchers explain how they choose the best models in this section. Models were chosen based on how well they performed given input parameters and how much they deviated from predictions of experiments. RMSE and  $R^2$  indicators are applied to determine the best models. The best models have the smallest RMSE and the highest  $R^2$  for all four sets of data (training, validating, testing, and all data). The behavior of models with parameters inputs is acceptable. In order to prevent overfitting, the best models should have a RMSE and a  $R^2$  that are as similar as possible for training, validating, testing, and all data. Overfitting is the large difference in error between training, validating, testing, and all data sets. Finally, the best models' performance is tested by comparison with design codes. There are six different codes that are used to evaluate how well models perform. The limitations of design codes were ignored during the comparison.

### 2.9. Graphical user interface

All interested users can benefit from using the graphical user interface to design, learn about, and understand the axial behavior of short rectangular CFST columns. Using the best models, a graphical user interface was created.

## 3. Results and discussion

This study designs a multi-fed forward back propagation and adaptive neuro fuzzy inference system for predicting ACC of short rectangular CFST columns. Two best models are selected, and their performance is evaluated. The models are compared to standard codes and a graphical user interface is created.

The RMSE and the  $R^2$  for multi fed forward back propagation neural network models are presented in Figure 8 (a) and (b), respectively. These models have a minimum RMSE from the one thousand models developed. MFFBPMModel7 was selected as the best model. MFFBPMModel7 has the minimum RMSE and a higher  $R^2$ . The RMSE and the  $R^2$  for adaptive neuro fuzzy inference system models may be seen in Figure 8 (c) and (d), respectively. These models have the lowest RMSE of the one hundred and twenty models developed. ANFISModel5 was selected as the best model. ANFISModel5 has the minimum RMSE and a higher  $R^2$ . Table 5 presents the RMSE and  $R^2$  for MFFBPMModel7 and ANFISModel5 models.

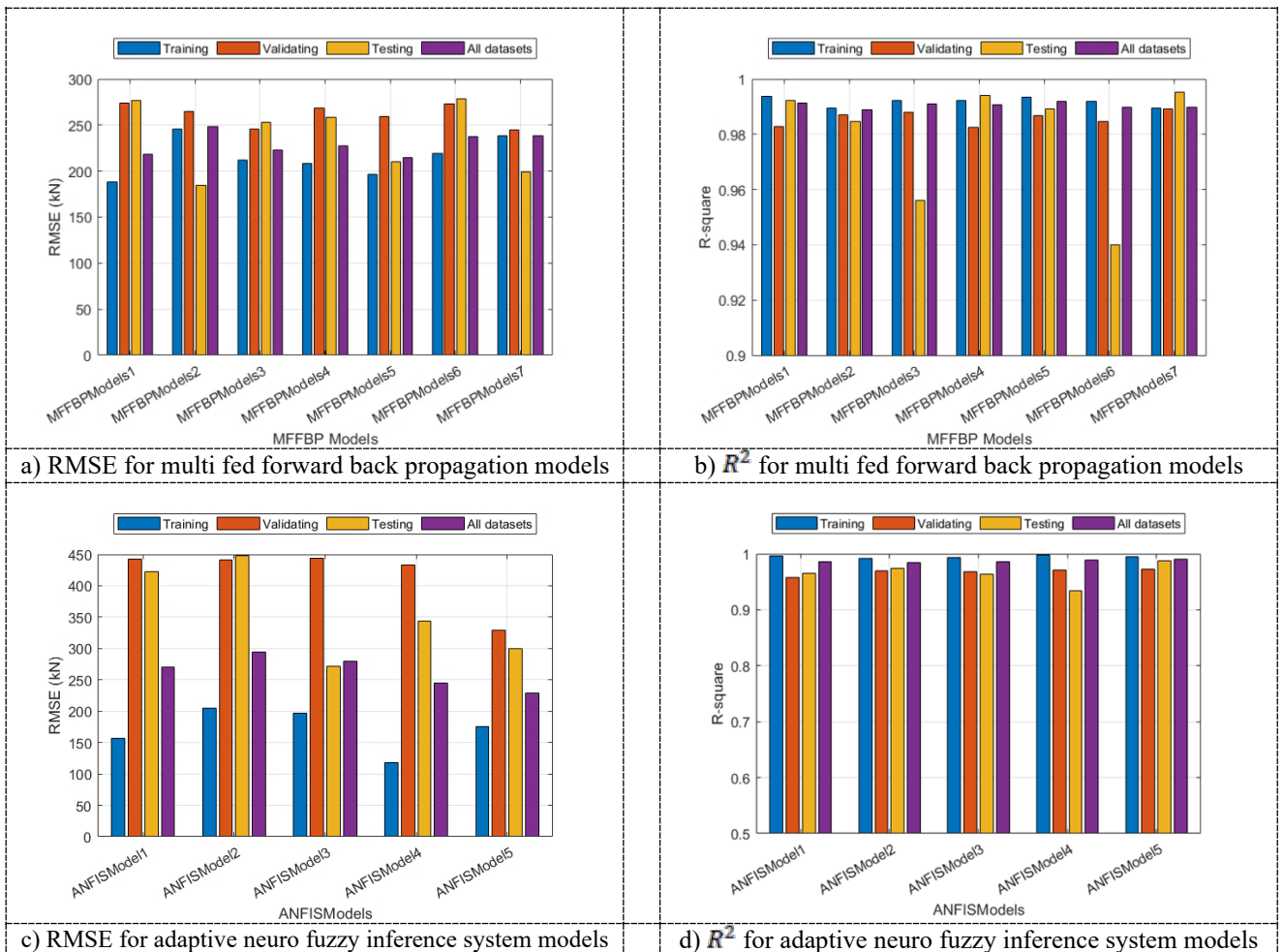


Fig. 8: Displays the RMSE and  $R^2$  for neural network and neural fuzzy models.

Figure 9 illustrates the training process of MFFBPMModel7 with the mean square error for training, validating, and testing. The best validation performance occurred at epoch 27, with a mean square error of 59775.45. Figure 10 illustrates the architecture of MFFBPMModel7. MFFBPMModel7 has four hidden layers: 35 neurons in the first, 15 in the second, 30 in the third, and 10 in the fourth. The activation function of hidden layers is softmax. Input parameters were width, height, tube thickness of steel, length, steel’s yield strength, concrete’s compressive strength, height to steel tube thickness ratio, and length to width ratio. Figure 11 shows the regression for MFFBPMModel7. The regression for MFFBPMModel7 is 0.994, 0.994, 0.997, and 0.994 for training, validating, testing, and all datasets, respectively. Higher regression was achieved with the experimental results.

The performance of ANFISModel5 is shown in Figure 12. There is good agreement with the experimental results, but some of the predicted values are less than zero. Figure 13 shows the regression of ANFISModel5. The regression for ANFISModel5 is 0.997, 0.986, 0.993, and 0.995 for training, validating, testing, and all datasets, respectively.

Higher regression was achieved with the experimental results. Figure 14 shows the behavior of MFFBPMModel7 with input parameters. The method used is to change the parameter within the range of experimental data, and other parameters are constant with the mean values of experimental data mentioned in Table 5. It is clear that with the increase in width, height, steel tube thickness, steel’s yield strength, and concrete’s compressive strength, the prediction model increases except that it decreases with increasing length [72].

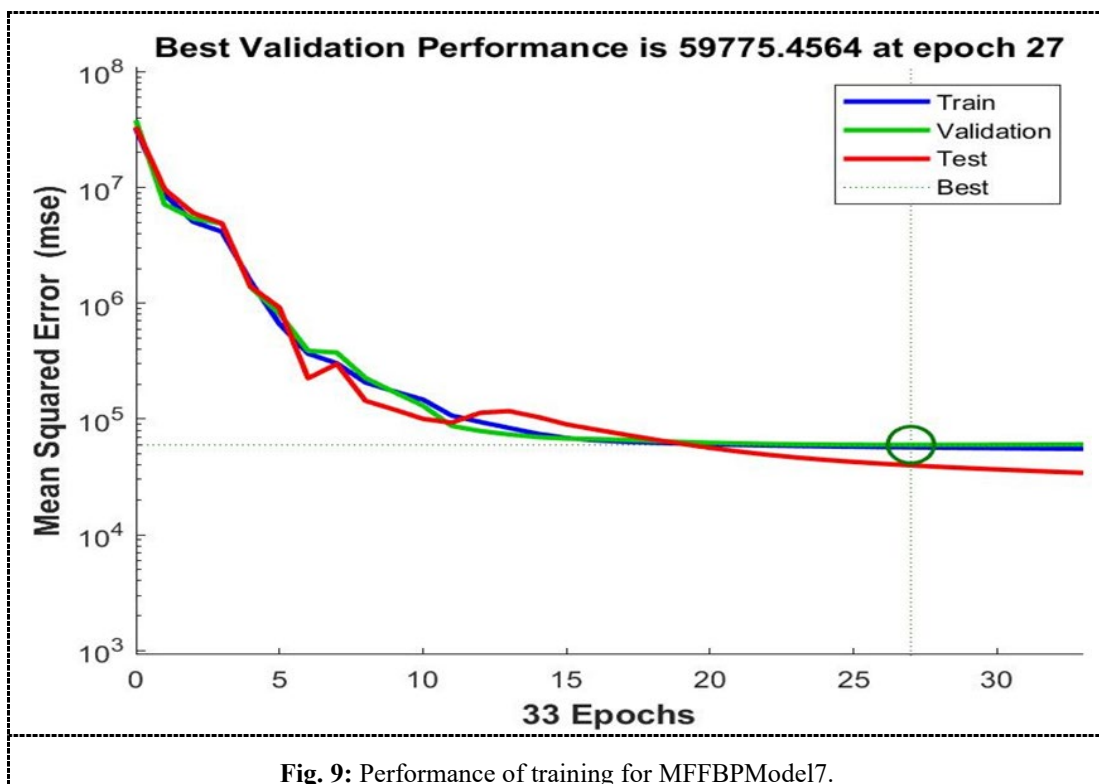


Fig. 9: Performance of training for MFFBPMModel7.

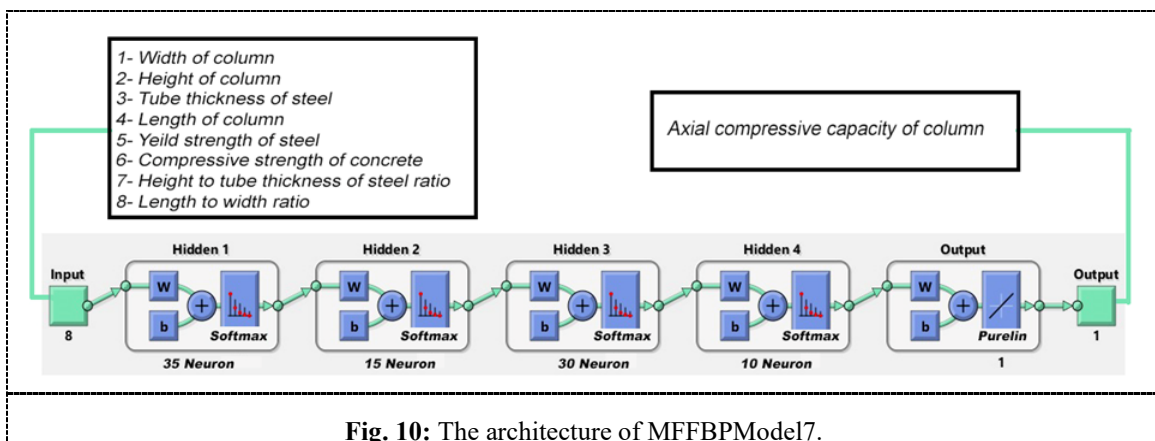


Fig. 10: The architecture of MFFBPMModel7.



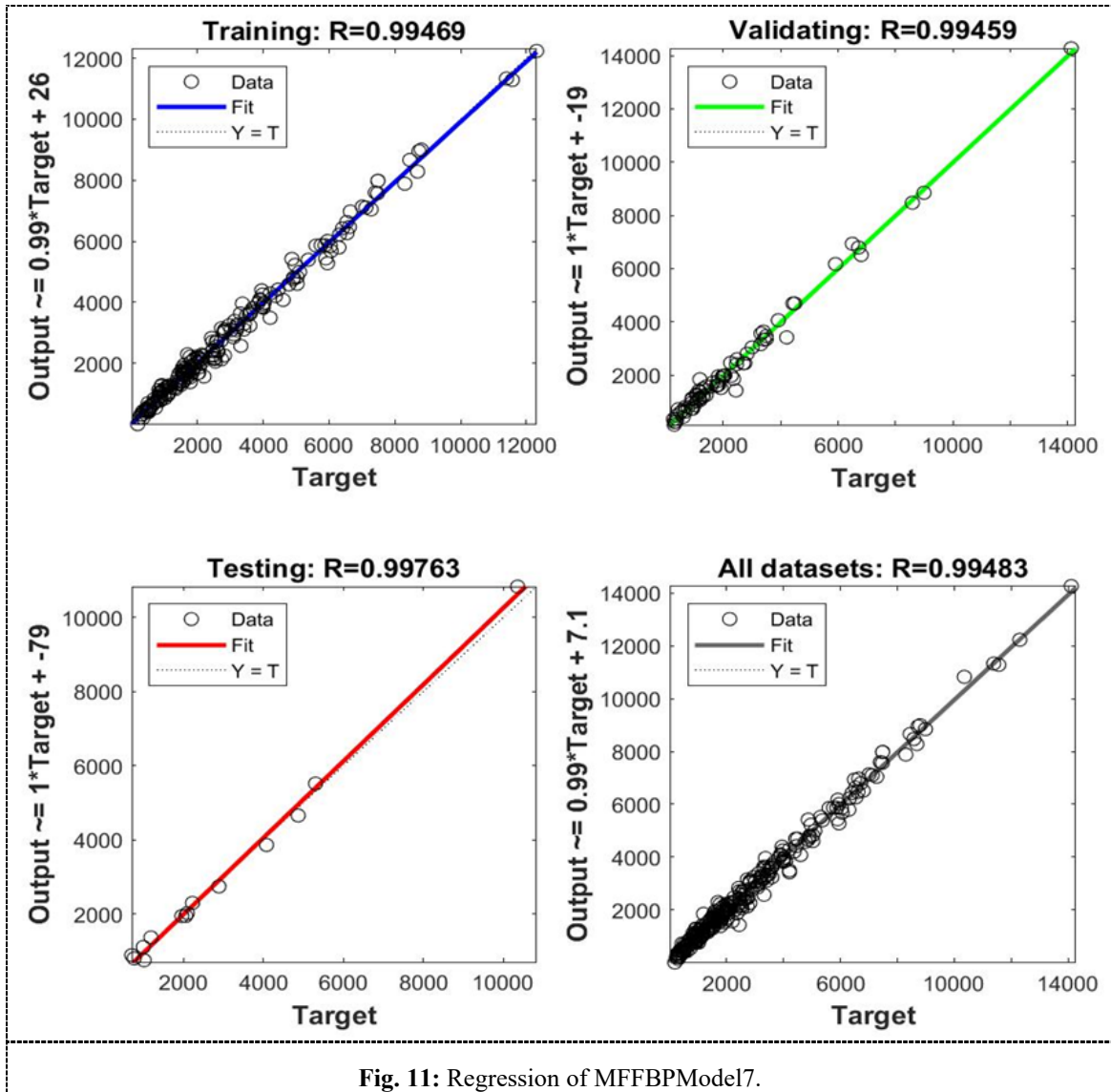


Fig. 11: Regression of MFFBPMModel7.

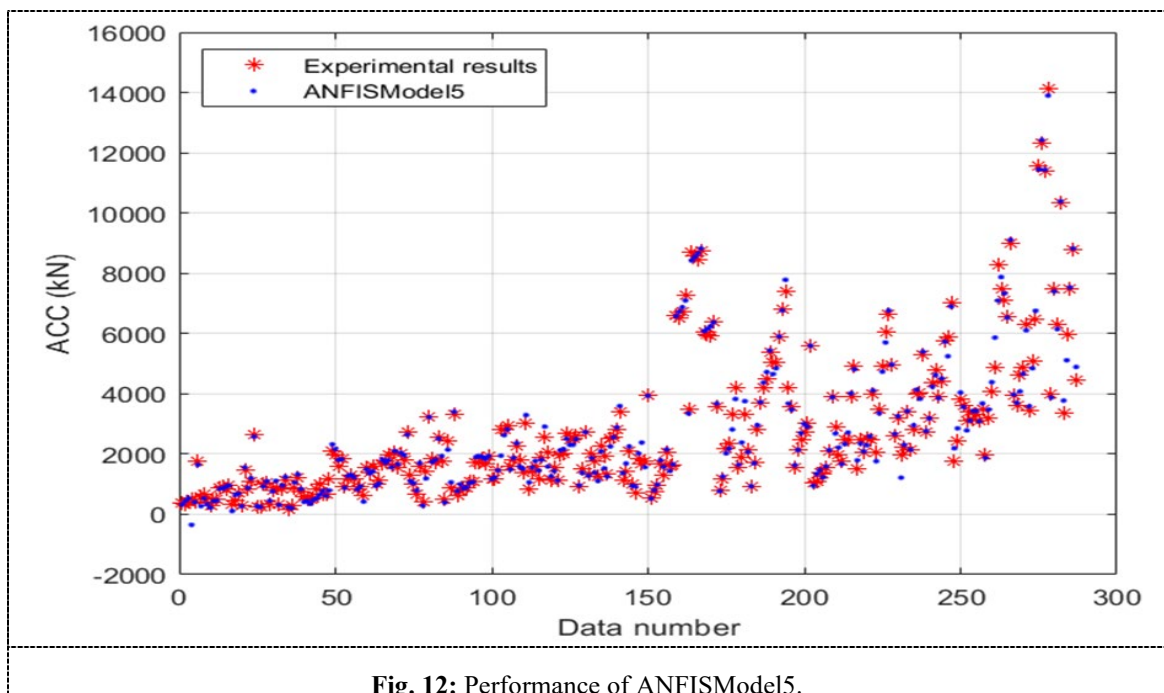
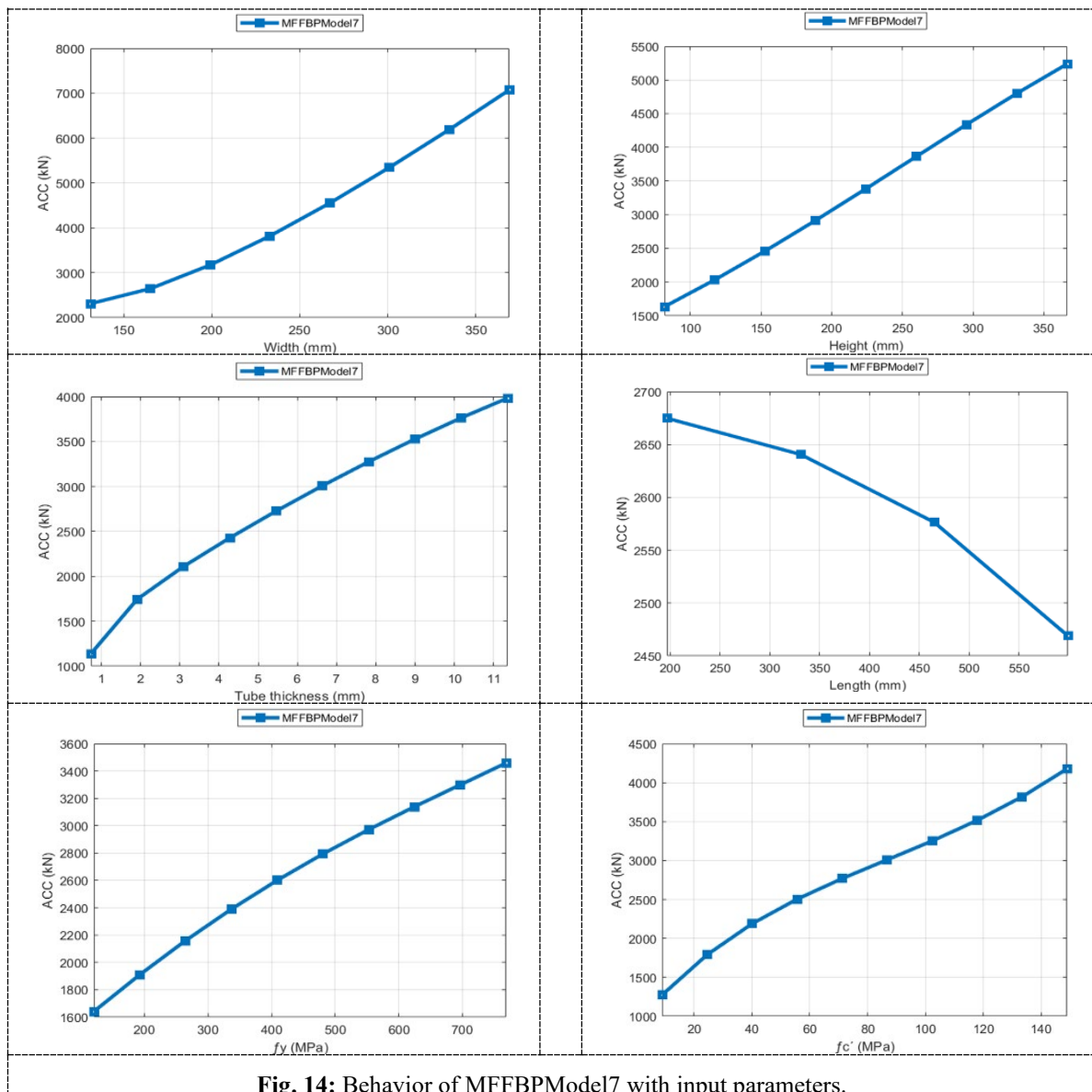
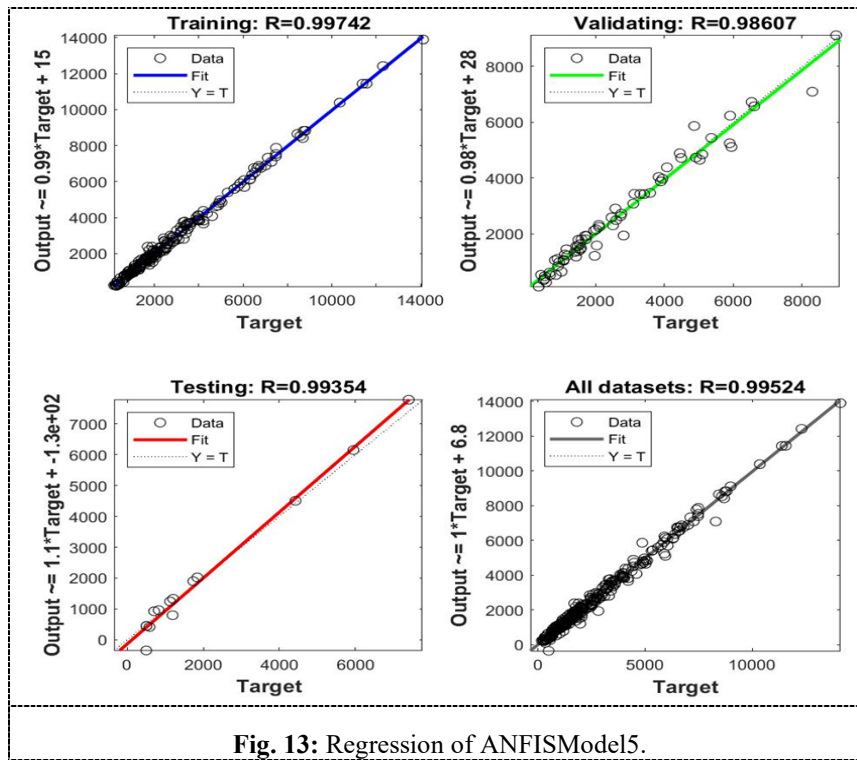


Fig. 12: Performance of ANFISModel5.





**Table 3:** The models' RMSE and  $R^2$ .

Model name	Training data		Validating data		Testing data		All datasets	
	RMSE	$R^2$	RMSE	$R^2$	RMSE	$R^2$	RMSE	$R^2$
MFFBPMModel7	238.30	0.9894	244.49	0.9892	199.30	0.9953	238.13	0.9897
ANFISModel5	176.04	0.9949	328.96	0.9723	299.22	0.9871	228.35	0.9905

Figure 15 illustrates the behavior of ANFISModel5 with input parameters. By using the same method mentioned above. It is clear that with an increase in height, tube thickness of steel, steel's yield strength, and concrete's compressive strength, the prediction model increases. It is observed that with increasing the width and length of the column, the model prediction increases, and after that, it decreases. Sometimes, model predictions give values less than zero. This means that the prediction model is not suitable for all applications for the prediction of the ACC of short rectangular CFST columns.

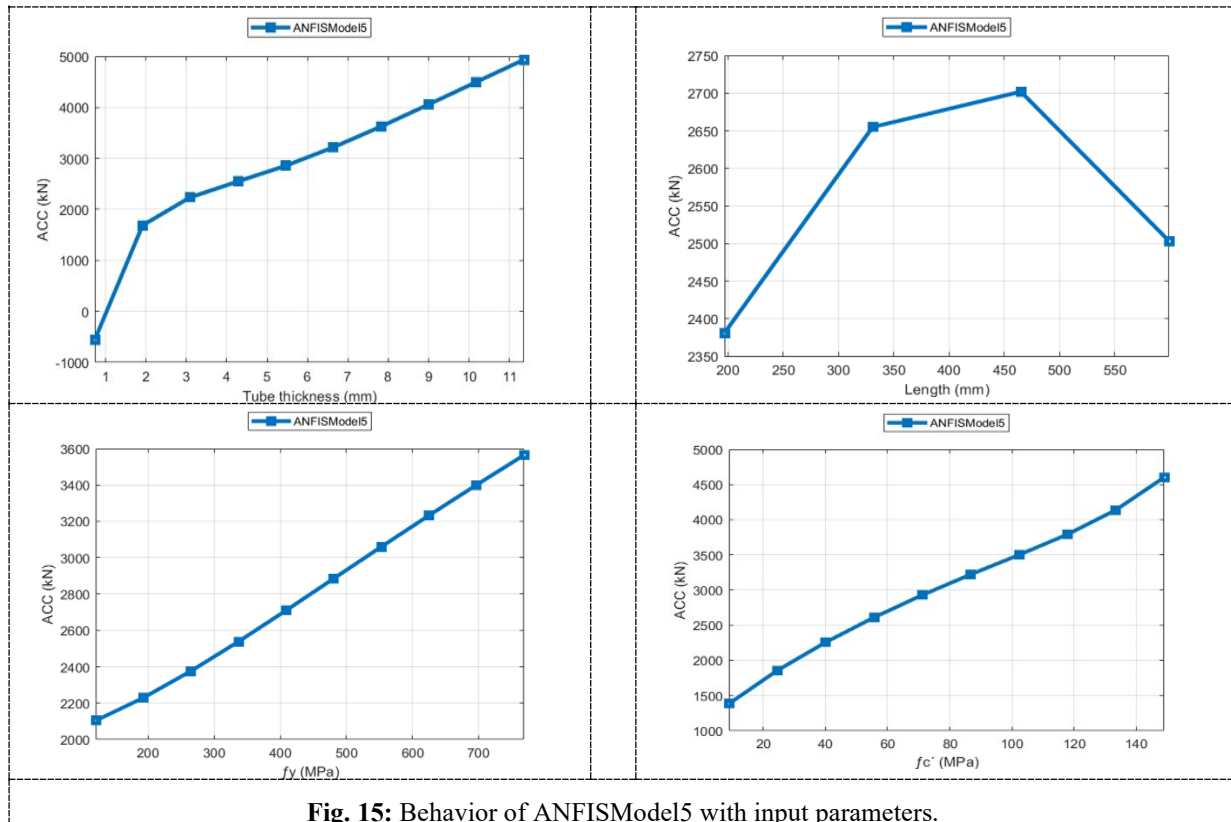
**Fig. 15:** Behavior of ANFISModel5 with input parameters.

Figure 16 shows the results for MFFBPMModel7, ANFISModel5, Eurocode4, AISC360, AS5100, ACI318, AIJ2001, and DBJ13-51 as a comparison with experimental results. The design codes are applied without safety factors and ignore the limitations mentioned in Table 6. By using all datasets, MFFBPMModel7 gives the best results, followed by ANFISModel5, but with some values less than zero. Figures 17, 18, and 19 present the comparison between MFFBPMModel7, ANFISModel5, and design codes. ANFISModel5 and MFFBPMModel7 have the least RMSE, a higher  $R^2$ , and the least MAPE. It followed by Eurocodes4 as performance index [73]. As a result, MFFBPMModel7 has good predictions for the ACC of short rectangular CFST columns. In order to facilitate comparison between different models and design codes, Table 6 provides the values of the RMSE,  $R^2$ , and MAPE.

MFFBPMModel7 has a strong agreement with experimental data and delivers the best results for the ACC of short rectangular CFST columns compared with ANFISModel5 and the formula of design codes, according to all of the results and comparisons that were described previously. Finally, as seen in Figure 20, the graphic user interface was created.

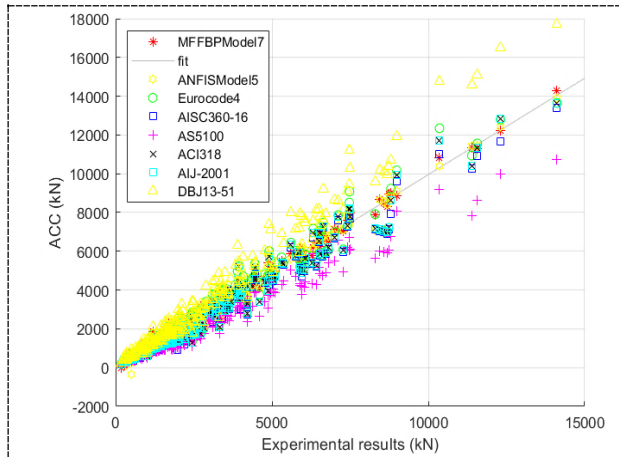


Fig. 16: Results of MFFBPMo del7, ANFISModel5 and design codes as comparison with experimental results.

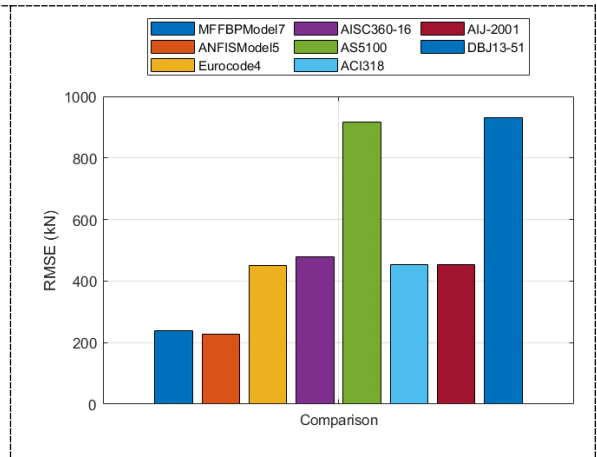


Fig. 17: RMSE comparison between MFFBPMo del7, ANFISModel5 and design codes.

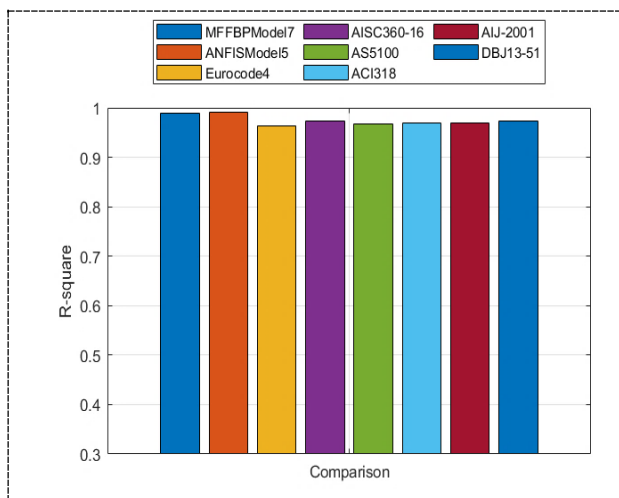


Fig. 18:  $R^2$  comparison between MFFBPMo del7, ANFISModel5 and design codes.

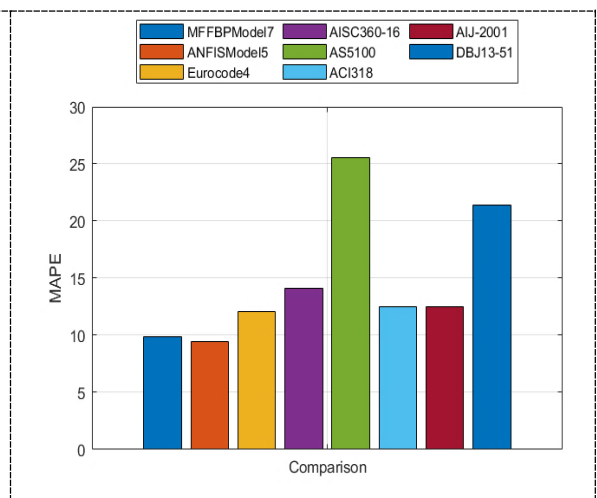


Fig. 19: MAPE comparison between MFFBPMo del7, ANFISModel5 and design codes.

Table 4: Comparison between models and design codes.

Type of statistical function	MFFBPMo del7	ANFIS Model5	Eurocode4	AISC360-16	AS5100	ACI318	AIJ-2001	DBJ13-51
RMSE	238.13	228.35	451.88	478.89	915.35	453.42	453.42	930.73
$R^2$	0.9897	0.9905	0.9643	0.9729	0.9680	0.9687	0.9687	0.9724
MAPE	9.88	9.46	12.05	14.10	25.53	12.53	12.53	21.41

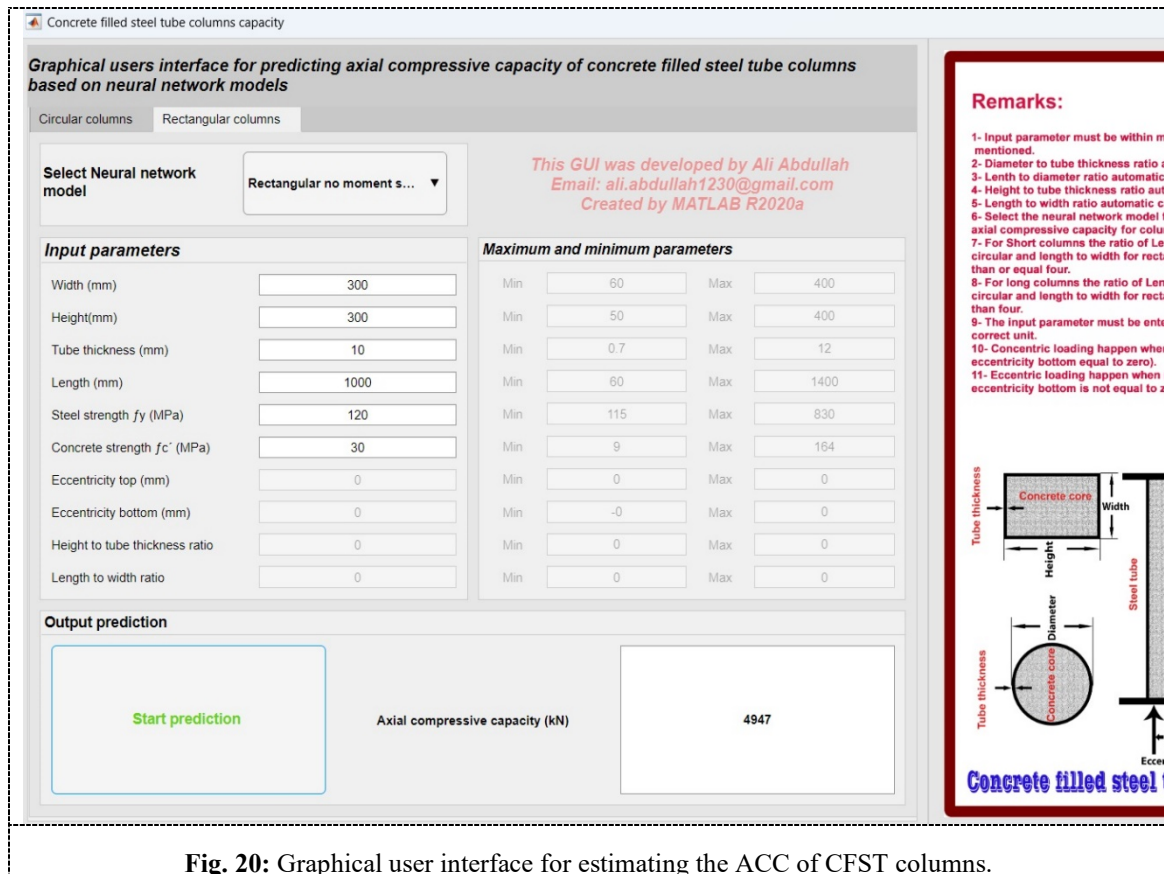


Fig. 20: Graphical user interface for estimating the ACC of CFST columns.

## 4. Conclusion and recommendations

### 4.1. Conclusion

Artificial neural network was used in this investigation to predict the ACC of short rectangular CFST columns. For this purpose, two type of neural network were used. The first one was a multi fed forward back propagation neural network. The second one was Sugeno type of adaptive neuro fuzzy inference system with Gaussian membership function and Subtractive Clustering to generate the rules for system.

A comparison of the two different kinds of artificial neural network models with the different prediction approaches design codes use. The results of this study have added to what was already known about how artificial neural network can be used to solve a specific control engineering problem. The new research is summarized in five points:

1. Generally, multi fed forward back propagation neural network model is more accurate in predicting the ACC of CFST columns when compared with the adaptive neuro fuzzy inference system model.
2. The RMSE and  $R^2$  results showed that multi fed forward back propagation neural network trained the using back propagation method could accurately estimate the ACC of rectangular CFST columns.
3. The behavior of multi fed forward back propagation neural network best model with input parameters changing within the range of datasets is acceptable when compared with the behavior of adaptive neuro fuzzy inference system best model.
4. The performance of the best model was noticeably better across the board, as measured by the various performance indices, including the RMSE, the  $R^2$ , and the MAPE when compared with design codes (Eurocode 4, AISC360-16, AS 5100, AIJ 2001, DBJ13-51, and ACI318).
5. The best models were used to construct the graphical user interface, which is now freely available to researchers, engineers, and interested individuals.

### 4.2. Recommendations

While this study has contributed to the existing body of knowledge in the field of artificial neural network for estimating the ACC of CFST columns, it is recommended that future research focus on the following activities:

1. Using genetic algorithm techniques to optimize the various parameters of artificial neural network models.
2. Alternatives to multi fed forward back propagation neural networks and adaptive neuro fuzzy inference system approaches for prediction, such as support vector machines and radial basis function networks, are being developed. These strategies could provide engineers with a wider range of options when solving engineering difficulties.

## Supplementary materials

All the data, results, models, information, and live script codes used in this study can be obtained by contacting the author by email at: ali.abdullah1230@gmail.com.

## References

- [1] Gourley BC, Tort C, Hajjar JF, Schiller PH, (2001), A synopsis of studies of the monotonic and cyclic behaviour of concrete-filled steel tube beam-columns. University of Minnesota Minneapolis
- [2] Elremaily A, Azizinamini A, (2002), "Behavior and strength of circular concrete-filled tube columns"
- [3] Shanmugam NE, Lakshmi B, (2001), "State of the art report on steel-concrete composite columns"
- [4] Knowles RB, Park R, (1970), "Axial load design for concrete filled steel tubes," *Journal of the Structural Division* 96:2125–2153
- [5] Tsuji B, (1991), "Axial compression behavior of concrete filled circular steel tubes" *Proceedings of the Third International Conference on Steel-Concrete Composite Structures*, 1991. 9
- [6] Zhong ST, (1991), "The Concrete Filled Steel Tubular (CFST) Structures in China" *the Third International Conference on Steel-Concrete Composite Structures*
- [7] Committee A, (2016), "Specification for structural steel buildings (ANSI/AISC 360-16)" *American Institute of Steel Construction Chicago*
- [8] Liu X, Liu J, Yang Y, Cheng G, Lartificial neural networking J, (2020), "Resistance of special-shaped concrete-filled steel tube columns under compression and bending," *J Constr Steel Res* 169:106038, <https://www.sciencedirect.com/science/article/pii/S0143974X19312611>
- [9] Han L-H, Li W, Bjorhovde R, (2014), "Developments and advanced applications of concrete-filled steel tubular (CFST) structures: Members," *J Constr Steel Res* 100:211–228, <https://www.sciencedirect.com/science/article/pii/S0143974X14000996>
- [10] Han L-H, (2002), "Tests on stub columns of concrete-filled RHS sections," *J Constr Steel Res* 58:353–372
- [11] Johansson M, (2004), "Composite action and confinement effects in tubular steel-concrete columns."
- [12] (Fred) Cha D, Zhang H, Blumenstein M, (2011), "Prediction of maximum wave-induced liquefaction in porous seabed using multi-artificial neural network model," *Ocean Engineering* 38:878–887, <https://www.sciencedirect.com/science/article/pii/S0029801810001848>
- [13] French MN, Krajewski WF, Cuykendall RR, (1992), "Rainfall forecasting in space and time using a neural network," *J Hydrol (Amst)* 137:1–31, <https://www.sciencedirect.com/science/article/pii/002216949290046X>
- [14] Kasperkiewicz J, Racz J, Dubrawski A, (1995), "HPC strength prediction using artificial neural network," *Journal of Computing in Civil Engineering* 9:279–284
- [15] Grubert JP, (1995), "Prediction of estuarine instabilities with artificial neural networks," *Journal of Computing in Civil Engineering* 9:266–274
- [16] Aziz HY, (2014), "Deep pile foundation settlement prediction using neurofuzzy networks" *The Open Civil Engineering Journal* 8:
- [17] Thirumalaiah K, Deo MC, (1998), "River stage forecasting using artificial neural networks," *J Hydrol Eng* 3:26–32
- [18] Deo MC, Kumar NK, (2000), "Interpolation of wave heights," *Ocean Engineering* 27:907–919, <https://www.sciencedirect.com/science/article/pii/S0029801899000232>
- [19] Jiang N, Zhao Z, Ren L, (2003), "Design of structural modular neural networks with genetic algorithm," *Advances in Engineering Software* 34:17–24, <https://www.sciencedirect.com/science/article/pii/S0965997802001072>
- [20] Jakubek SM, Strasser TI, (2004), "Artificial neural networks for fault detection in large-scale data acquisition systems," *Eng Appl Artif Intell* 17:233–248, <https://www.sciencedirect.com/science/article/pii/S0952197604000223>
- [21] Zhao Z, (2006), "Steel columns under fire—a neural network based strength model," *Advances in Engineering Software* 37:97–105, <https://www.sciencedirect.com/science/article/pii/S0965997805000852>
- [22] Armaghani DJ, Mohamad ET, Narayanasamy MS, Narita N, Yagiz S, (2017), "Development of hybrid intelligent models for predicting TBM penetration rate in hard rock condition," *Tunnelling and Underground Space Technology* 63:29–43, <https://www.sciencedirect.com/science/article/pii/S0886779815303473>
- [23] Chen W, Sarir P, Bui X-N, Nguyen H, Tahir MM, Jahed Armaghani D, (2020), "Neuro-genetic, neuro-imperialism and genetic programming models in predicting ultimate bearing capacity of pile," *Eng Comput* 36:1101–1115, <https://doi.org/10.1007/s00366-019-00752-x>
- [24] Parsajoo M, Armaghani DJ, Mohammed AS, Khari M, Jahandari S, (2021), "Tensile strength prediction of rock material using non-destructive tests: A comparative intelligent study," *Transportation Geotechnics* 31:100652, <https://www.sciencedirect.com/science/article/pii/S2214391221001422>
- [25] Du C, Liu X, Liu Y, Tong T, (2021), "Prediction of the Interface Shear Strength between Ultra-High-Performance Concrete and Normal Concrete Using Artificial Neural Networks," *Materials* 14:5707
- [26] Kovačević M, Lozančić S, Nyarko EK, Hadzima-Nyarko M, (2021), "Modeling of compressive strength of self-compacting rubberized concrete using machine learning," *Materials* 14:4346
- [27] Li C, Zhou J, Armaghani DJ, Li X, (2021), "Stability analysis of underground mine hard rock pillars via combination of finite difference methods, neural networks, and Monte Carlo simulation techniques," *Underground Space* 6:379–395, <https://www.sciencedirect.com/science/article/pii/S2467967420300441>
- [28] Asteris PG, Koopialipoor M, Armaghani DJ, Kotsonis EA, Lourenço PB, (2021), "Prediction of cement-based mortars compressive strength using machine learning techniques," *Neural Comput Appl* 33:13089–13121, <https://doi.org/10.1007/s00521-021-06004-8>
- [29] Nguyen N-H, Vo TP, Lee S, Asteris PG, (2021), "Heuristic algorithm-based semi-empirical formulas for estimating the compressive strength of the normal and high performance concrete," *Constr Build Mater* 304:124467, <https://www.sciencedirect.com/science/article/pii/S0950061821022248>
- [30] Armaghani DJ, Harandizadeh H, Momeni E, Maizir H, Zhou J, (2022), "An optimized system of GMDH-ADAPTIVE NEURO FUZZY INFERENCE SYSTEM predictive model by ICA for estimating pile bearing capacity," *Artif Intell Rev* 55:2313–2350, <https://doi.org/10.1007/s10462-021-10065-5>
- [31] Asteris PG, Rizal FIM, Koopialipoor M, Roussis PC, Ferentinou M, Armaghani DJ, Gordan B, (2022), "Slope stability classification under seismic conditions using several tree-based intelligent techniques," *Applied Sciences* 12:1753

- [32] Asteris PG, Lourenço PB, Roussis PC, et al, (2022), "Revealing the nature of metakaolin-based concrete materials using artificial intelligence techniques," *Constr Build Mater* 322:126500, <https://www.sciencedirect.com/science/article/pii/S0950061822001921>
- [33] Khajehzadeh M, Keawsawasvong S, Sarir P, Khailany DK, (2022), "Seismic analysis of earth slope using a novel sequential hybrid optimization algorithm," *Periodica Polytechnica Civil Engineering* 66:355–366
- [34] Moon J, Kim JJ, Lee T-H, Lee H-E, (2014), "Prediction of axial load capacity of stub circular concrete-filled steel tube using fuzzy logic," *J Constr Steel Res* 101:184–191, <https://www.sciencedirect.com/science/article/pii/S0143974X14001461>
- [35] Ahmadi M, Naderpour H, Kheyroddin A, (2014), "Utilization of artificial neural networks to prediction of the capacity of CCFT short columns subject to short term axial load," *Archives of Civil and Mechanical Engineering* 14:510–517, <https://www.sciencedirect.com/science/article/pii/S1644966514000089>
- [36] Ahmadi M, Naderpour H, Kheyroddin A, (2017), "ARTIFICIAL NEURAL NETWORK Model for Predicting the Compressive Strength of Circular Steel-Confined Concrete," *International Journal of Civil Engineering* 15:213–221, <https://doi.org/10.1007/s40999-016-0096-0>
- [37] Du Y, Chen Z, Zhang C, Cao X, (2017), "Research on axial bearing capacity of rectangular concrete-filled steel tubular columns based on artificial neural networks," *Front Comput Sci* 11:863–873
- [38] Jayalekshmi S, Jegadesh JSS, Goel A, (2018), "Empirical Approach for Determining Axial Strength of Circular Concrete Filled Steel Tubular Columns," *Journal of The Institution of Engineers (India): Series A* 99:257–268
- [39] Tran VL, Thai DK, Kim SE, (2019), "Application of ARTIFICIAL NEURAL NETWORK in predicting ACC of SCFST column" *Compos Struct*. <https://doi.org/10.1016/j.compstruct.2019.111332>
- [40] Tran V-L, Thai D-K, Nguyen D-D, (2020), "Practical artificial neural network tool for predicting the axial compression capacity of circular concrete-filled steel tube columns with ultra-high-strength concrete," *Thin-Walled Structures* 151:106720, <https://www.sciencedirect.com/science/article/pii/S0263823119314867>
- [41] Zarringol M, Thai HT, Thai S, Patel V, (2020), "Application of ARTIFICIAL NEURAL NETWORK to the design of CFST columns," *Structures* 28:2203–2220
- [42] Asteris PG, Lemonis ME, Le T-T, Tsavdaridis KD, (2021), "Evaluation of the ultimate eccentric load of rectangular CFSTs using advanced neural network modeling," *Eng Struct* 248:113297, <https://www.sciencedirect.com/science/article/pii/S0141029621014164>
- [43] Sarir P, Shen SL, Wang ZF, Chen J, Horpibulsuk S, Pham BT, (2021), "Optimum model for bearing capacity of concrete-steel columns with AI technology via incorporating the algorithms of IWO and ABC," *Eng Comput* 37:797–807
- [44] Le TT, Asteris PG, Lemonis ME, (2021), "Prediction of axial load capacity of rectangular concrete-filled steel tube columns using machine learning techniques" *Eng Comput*. <https://doi.org/10.1007/s00366-021-01461-0>
- [45] Luat N-V, Shin J, Lee K, (2022), "Hybrid BART-based models optimized by nature-inspired metaheuristics to predict ultimate axial capacity of CCFST columns," *Eng Comput* 38:1421–1450, <https://doi.org/10.1007/s00366-020-01115-7>
- [46] Mai SH, Ben Seghier MEA, Nguyen PL, Jafari-Asl J, Thai D-K, (2022), "A hybrid model for predicting the axial compression capacity of square concrete-filled steel tubular columns," *Eng Comput* 38:1205–1222, <https://doi.org/10.1007/s00366-020-01104>
- [47] Avci-Karatas C, (2022), "Artificial Neural Network (ARTIFICIAL NEURAL NETWORK) Based Prediction of Ultimate Axial Load Capacity of Concrete-Filled Steel Tube Columns (CFSTCs)," *International Journal of Steel Structures* 22:1341–1358
- [48] Wang C, Chan T-M, (2023), "Machine learning (ML) based models for predicting the ultimate strength of rectangular concrete-filled steel tube (CFST) columns under eccentric loading," *Eng Struct* 276:115392, <https://www.sciencedirect.com/science/article/pii/S0141029622014687>
- [49] Duong TH, Le T-T, Le M V, (2023), "Practical Machine Learning Application for Predicting Axial Capacity of Composite Concrete-Filled Steel Tube Columns Considering Effect of Cross-Sectional Shapes," *International Journal of Steel Structures* 23:263–278, <https://doi.org/10.1007/s13296-022-00693-0>
- [50] Zhou X-G, Hou C, Feng W-Q, (2023), "Optimized data-driven machine learning models for axial strength prediction of rectangular CFST columns," *Structures* 47:760–780, <https://www.sciencedirect.com/science/article/pii/S2352012422010694>
- [51] En BS, (2004), "1-1. Eurocode 2: Design of concrete structures—Part 1-1: General rules and rules for buildings"
- [52] Committee ACI, (2014), "Building code requirements for structural concrete:(ACI 318-14) and commentary (ACI 318R-14)" American Concrete Institute
- [53] AIJ B, (2001), "Recommendations for design and construction of concrete filled steel tubular structures"
- [54] DBJ13-51-2010, (2010), "Technical Specification for Concrete-filled Steel Tubular Structures" The Department of Housing and Urban-Rural Development of Fujian Province ...
- [55] Standard A, (2004), "AS5100. 2-2004, Bridge design—Part 6: Steel and composite construction"
- [56] Gourley BC, Hajjar JF, (1994), "Cyclic nonlinear analysis of three-dimensional concrete-filled steel tube beam-columns and composite frames" Rep. No. ST-94 3:
- [57] Zhang W, Shahrooz BM, (1999), "Strength of short and long concrete-filled tubular columns," *Structural Journal* 96:230–238
- [58] Inai E, Sakino K, (1996), "Simulation of flexural behavior of square concrete filled steel tubular columns" Proc., 3rd Joint Technical Coordinating Committee Meeting, US-Japan Cooperative Research Program, Phase 5: Composite and Hybrid Structures
- [59] Sakino K, (1998), "Experimental studies and design recommendations on concrete filled steel tubular columns-US-Japan Cooperative Earthquake Research Program" Structural Engineering World Conference
- [60] Chauvin Y, Rumelhart DE, (2013), *Backpropagation: theory, architectures, and applications*. Psychology press
- [61] Naderpour H, Kheyroddin A, Amiri GG, (2010), "Prediction of FRP-confined compressive strength of concrete using artificial neural networks," *Compos Struct* 92:2817–2829, <https://www.sciencedirect.com/science/article/pii/S026382310001443>
- [62] Cilimkovic M, (2015), "Neural networks and back propagation algorithm" Institute of Technology Blanchardstown, Blanchardstown Road North Dublin 15:
- [63] Rutkowska D, (2002), "Neuro-Fuzzy Architectures and Hybrid Learning. Heidelberg, New York: Physica"
- [64] Lin C-T, Lee CSG, (1996), *Neural fuzzy systems: a neuro-fuzzy synergism to intelligent systems*. Prentice-Hall, Inc.
- [65] Jang J-S, (1993), "ADAPTIVE NEURO FUZZY INFERENCE SYSTEM : adaptive-network-based fuzzy inference system," *IEEE Trans Syst Man Cybern* 23:665–685
- [66] Thai H-T, Thai S, Ngo T, Uy B, Kang WH, Hicks SJ, (2020), "Concrete-filled steel tubular (CFST) columns database with 3,208 tests" <https://doi.org/10.17632/J3F5CX9YJH.1>
- [67] L'Hermite R, (1955), *Idées actuelles sur la technologie du béton. La Documentation technique du bâtiment et des travaux publics*



- [68] Thai S, Thai H-T, Uy B, Ngo T, (2019), "Concrete-filled steel tubular columns: Test database, design and calibration," *J Constr Steel Res* 157:161–181, <https://www.sciencedirect.com/science/article/pii/S0143974X1831321X>
- [69] Hudson M, Martin B, Hagan T, Demuth R2017b HB, (1992), "Neural Network Toolbox TM User's Guide"
- [70] Baum E, Haussler D, (1988), "What size net gives valid generalization?" *Adv Neural Inf Process Syst* 1:
- [71] Jang J-SR, Gulley N, (1995), "Fuzzy logic toolbox user's guide," The Mathworks Inc 1:19
- [72] Han L-H, Yao G-H, (2003), "Behaviour of concrete-filled hollow structural steel (HSS) columns with pre-load on the steel tubes," *J Constr Steel Res* 59:1455–1475, <https://www.sciencedirect.com/science/article/pii/S0143974X03001020>
- [73] Liu D, Gho W-M, Yuan J, (2003), "Ultimate capacity of high-strength rectangular concrete-filled steel hollow section stub columns," *J Constr Steel Res* 59:1499–1515, <https://www.sciencedirect.com/science/article/pii/S0143974X03001068>